Powder Metallurgy and Metal Ceramics, Vol. 34, Nos. 11-12, 1995

POWDER-MATERIAL RESEARCH METHODS AND PROPERTIES

POLYTHERMAL SECTIONS OF THE $Al_2O_3-ZrO_2-Y_2O_3$ PHASE DIAGRAM

S. N. Lakiza, L. M. Lopato, and I. E. Kir'yakova

UDC 546-31:621:641:831

Polythermal sections of the $Al_2O_3-ZrO_2-Y_2O_3$ phase diagram confirm that the system is quasibinary and enable one to give a complete phase diagram for the system. The ternary eutectic Al_2O_3 + ZrO_2 (solid solution) + $Y_3Al_5O_{12}$ has the lowest melting point in the system, whose temperature is 1715°C. No single-phase regions for the ternary solid solutions have been identified, which indicates that Al_2O_3 is not soluble in solid solutions based on F-ZrO_2 and C-Y_2O_3. This gives theoretical evidence for the scope for making new ceramics in this ternary system, which may have a high level of mechanical characteristics.

Materials in the $Al_2O_3-ZrO_2-Y_2O_3$ system have high values for the viscosity and strength in the family of high-technology ceramics. Elements of the phase diagram for this system have been researched in [1-7]. Data on the binary bounding systems have been taken from [8-21].

Our purpose was to construct polythermal sections of the $Al_2O_3-ZrO_2-Y_2O_3$ phase diagram in order to represent it more fully. We chose three sections: along the 15 mol.% ZrO_2 isoconcentrate (15Z); for 50 mol.% Al_2O_3·50 mol.% ZrO_2 (50A·50Z)$-Y_2O_3$; and ZrO_2-YAlO_3 (YA). The initial substances and the experimental methods have been described in [5].

The 15Z isoconcentrate (Fig. 1) intersects four primary crystallization fields: those for the phases Al_2O_3 (A), $Y_3Al_5O_{12}(Y_3A_5)$ and for solid solutions based on the fluorite-type structure of ZrO_2 (F) with various Y_2O_3 (C). The solidus surface in the section is complicated. The section intersects five isothermal planes corresponding to one peritectic (L_p + T $\Leftrightarrow$ F + A, where T represents solid solutions based on the tetragonal form of ZrO_2 with various Y_2O_3 contents) and four eutectic ones ($L_{E1} \Leftrightarrow Y_2A + F + C$, $L_{E2} \Leftrightarrow Y_2A + F + YA$, $L_{E3} \Leftrightarrow YA + F + Y_3A_5$, $L_{E4} \Leftrightarrow Y_3A_5 + F + A$, where $Y_2A \Leftrightarrow Y_4Al_2O_9$), which are nonvariant equilibria, and also lineated crystallization surfaces for six (out of eleven) binary eutectics: $L \Leftrightarrow C + Y_2A$, $L \Leftrightarrow Y_2A + F$, $L \Leftrightarrow YA + F$, $L \Leftrightarrow Y_3A_5 + F$, $L \Leftrightarrow A + F$ and $L \Leftrightarrow A + T$, whose crystallization volumes lie between the liquidus and solidus surfaces for the $Al_2O_3-ZrO_2-Y_2O_3$ system. The polymorphic transition in Y_2O_3 (H $\Leftrightarrow$ C) occurs at 2350°C, which is close to the eutectic in the $ZrO_2-Y_2O_3$ system (2360°C). The 15Z isoconcentrate intersects all three partially quasibinary sections in the ternary system, and the widths of the two-phase regions for these are seen in Fig. 1a.

Parts a-c of Fig. 2 show heating curves for certain alloys in the 15 mol.% ZrO_2 isoconcentrate section, while Fig. 3 shows the microstructures.

The 50A·50Z$-Y_2O_3$ section intersects four primary crystallization fields: T, F, C, and H phases (Fig. 1b). The solidus surface is complicated, as is the 15 mol.% ZrO_2 isoconcentrate (Fig. 1a). The section intersects five isothermal planes corresponding to one peritectic nonvariant equilibrium P and four eutectic ones E_1, E_2, E_3, and E_4, and also lineated surfaces for the end of crystallization of the binary eutectics C + Y_2A, Y_2A + F, YA + F, Y_3A_5 + F, A + F. The A + T section between the liquidus and solidus surfaces in the ternary system intersects the crystallization volumes for eight binary eutectics: $L \Leftrightarrow C + Y_2A$, $L \Leftrightarrow Y_2A + F$, $L \Leftrightarrow Y_3A_5 + F$, $L \Leftrightarrow T + F$, $L \Leftrightarrow F + C$, $L \Leftrightarrow YA + F$, $L \Leftrightarrow A + F$, $L \Leftrightarrow T + A$.

This section differs from the 15Z isoconcentrate section in that instead of the crystallization volume for the Y_3A_5 + A binary eutectic it intersects the same volume for T + F. It is formed by connode triangles based on the equilibrium T and F phases, whose compositions lie near the ZrO_2 vertex and migrate along the curves T'T" and F'F", while the compositions of the liquid migrate along the monovariant equilibrium line m_2P [7], Fig. 1a. At the temperature of the peritectic four-phase

Materials Science Institute, Ukrainian National Academy of Sciences, Kiev. Translated from Poroshkovaya Metallurgiya, Nos. 11-12(382), pp. 74-79, November-December, 1995. Original article submitted February 25, 1993.

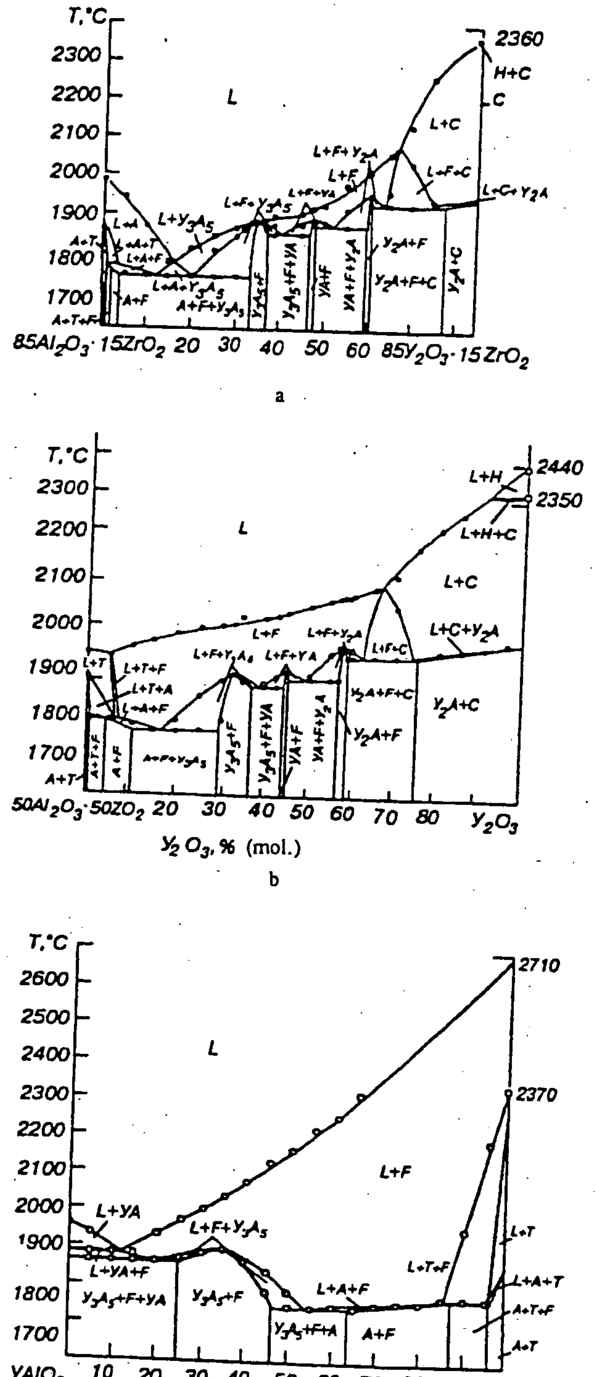

Fig. 1. Polythermal sections of the $Al_2O_3-ZrO_2-Y_2O_3$ phase diagram: a) 15 ZrO_2; b) 50 Al_2O_3·50 $ZrO_2-Y_2O_3$; c) ZrO_2-YAlO_3.

equilibrium $L_p + T \Leftrightarrow F + A$ (1745°C), the connode triangle lies in this plane and is part of it [7], region PT_2F_2 in Fig. 1a. Yttrium oxide undergoes a polymorphic transition at about 2350°C in a volume resembling a lobe in form and separating the regions of coexistence for liquid and H crystals (high-temperature solid solutions) and C (low-temperature ones). Below the solidus temperature, the section intersects three-phase regions separated by narrow two-phase regions, apart from the regions A + F and Y_3A_5 + F, which have appreciable widths.

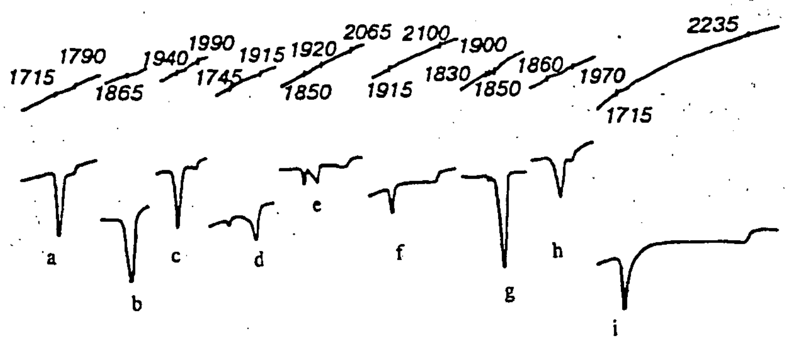

Fig. 2. Heating curves for alloys in polythermal sections of the $Al_2O_3-ZrO_2-Y_2O_3$ phase diagram. 15 ZrO_2 isoconcentrate: a) 20 Y_2O_3; b) 36 Y_2O_3; c) 60.5 Y_2O_3. Section 50 $Al_2O_3 \cdot 50$ $ZrO_2-Y_2O_3$: d) 5 Y_2O_3; e) 55 Y_2O_3; f) 65 Y_2O_3. Section ZrO_2-YAlO_3: g) 5 ZrO_2; h) 30 ZrO_2; i) 60 ZrO_2.

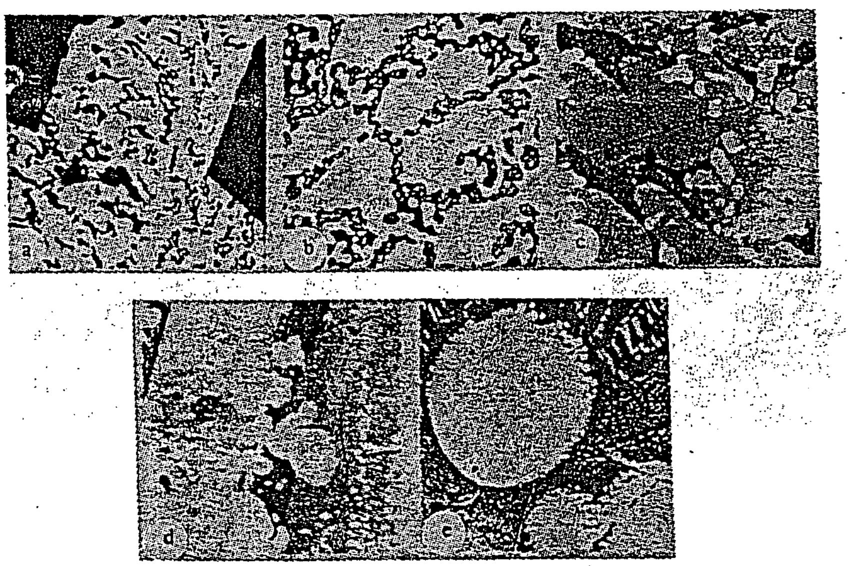

Fig. 3. Structure of alloys on the 15 ZrO_2 isoconcentrate for the $Al_2O_3-ZrO_2-Y_2O_3$ phase diagram. Y_2O_3 in mol.%: a) 15 (A, A + F + Y_3A_5); b) 20 (Y_3A_5, A + F + Y_3A_5); c) 43 (F, F + YA, Y_3A_5 + F + YA); d) 56(F, F + Y_2A, YA + F + Y_2A); e) 70 (C, C + F, Y_2A + F + C); magnifications: a) 2000; b) 700; c and e) 1000; d) 800.

Parts d-f of Fig. 2 show heating curves for alloys in the 50A:50Z$-Y_2O_3$ section, while Fig. 4 shows the microstructures.

The ZrO_2-YA section (Fig. 1c) indicates the structure of the $Al_2O_3-ZrO_2-Y_2O_3$ phase diagram at the ZrO_2 vertex. That section intersects two primary crystallization fields: YA and F. The solidus surface for this section is simpler than those for the two previous sections. The section intersects three isothermal planes corresponding to one peritectic nonvariant equilibrium P and two eutectic ones E_3 and E_4, and also the lineated surfaces for the end of crystallization for the three binary eutectics Y_3A_3 + F, A + F and A + T, whose crystallization volumes lie between the liquidus and solidus surfaces in the $Al_2O_3-ZrO_2-Y_2O_3$ system. The temperature of the polymorphic transition in ZrO_2 (T⇔F) falls smoothly as the Y_2O_3 content increases from 2370 to 1745°C, the temperature of the four-phase peritectic transformation L_p + T ⇔ F + C. Below the solidus temperatures, the ZrO_2-YA section intersects three three-phase regions separated by corresponding broad two-phase regions.

Parts g-i of Fig. 2 show the heating curves for certain alloys in the ZrO_2-YA section, while Fig. 5 shows the microstructures.

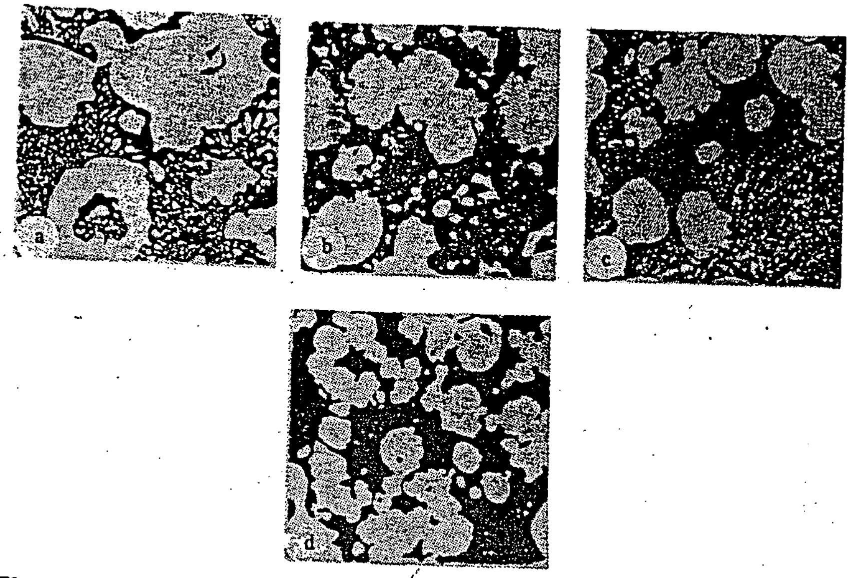

Fig. 4. Electron micrographs of certain alloys in the 50 $Al_2O_3 \cdot 50$ $ZrO_2-Y_2O_3$ polythermal section for the $Al_2O_3-ZrO_2-Y_2O_3$ phase diagram, $\times 1000$. Y_2O_3 contents in mol.%: a) 3 (T, A + T + F); b) 12 (F, A +F, eutectic A + F + Y_3A_5); c) 20 (F, F + Y_3A_5, A + F + Y_3A_5 eutectic); d) 65 (F, F + C, Y_2A + F + C eutectic).

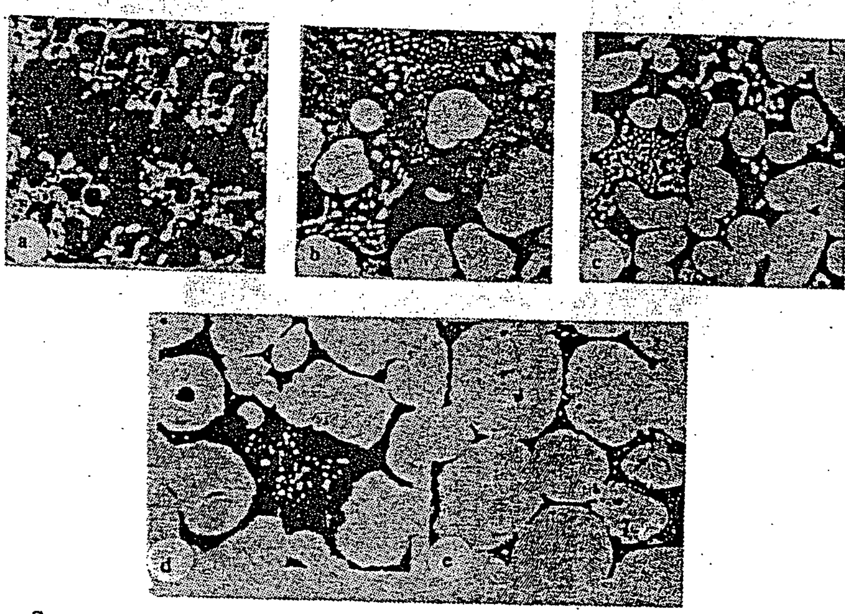

Fig. 5. Structures of alloys in the ZrO_2-YAlO_3 polythermal section of the $Al_2O_3-ZrO_2-Y_2O_3$ phase diagram. ZrO_2 in mol.%: a) 10 (YA, YA + F, Y_3A_5 + F + YA); b) 22 (F, Y_3A_5 + F, Y_3A_5 + F + YA); c) 35 (F, Y_3A_5 + F); d) 60 (F, F + A, A + F + Y_3A_5); e) 80 (F, A + F). Magnifications: a) 600; b) 2000; c and d) 1000; e) 700.

These polythermal sections for the $Al_2O_3-ZrO_2-Y_2O_3$ system confirm that the sections examined in [5] are quasibinary. Together with the [5, 7] data, they give the complete phase diagram. The low melting point (1715°C) occurs for the Al_2O_3 + F + $Y_3Al_5O_{12}$ ternary eutectic. Single-phase regions for the ternary solid solutions are not observed, which shows that Al_2O_3 is not soluble in the F and C solid solutions. This is the theoretical basis for making new ceramics in this ternary system with a high level of mechanical properties.

REFERENCES

1. W. D. and T. Y. Tien, "Subsolidus phase equilibria in the $ZrO_2-Y_2O_3-Al_2O_3$ system," J. Amer. Ceram. Soc., **63**, No. 9-10, 595-596 (1980).
2. S. G. Popov, S. F. Pashin, M. V. Paromova, et al., "Subsolidus phase equilibria in the $ZrO_2-Y_2O_3-Al_2O_3$ system," Izv. AN SSSR, Neorgan. Mater., **26**, No. 1, 113-117 (1990).
3. L. M. Lopato, L. V. Nazarenko, G. I. Gerasimyuk, et al., "Interactions in the $ZrO_2-Y_2O_3-Al_2O_3$ system at 1650°C," Ibid., No. 4, 834-838.
4. L. M. Lopato, L. V. Nazarenko, G. I. Gerasimyuk, et al., "The isothermal section of the $ZrO_2-Y_2O_3-Al_2O_3$ phase diagram at 1250°C," Ibid., **28**, No. 4, 835-839 (1992).
5. S. N. Lakiza, L. M. Lopato, and A. V. Shevchenko, "Interactions in the $Al_2O_3-ZrO_2-Y_2O_3$ system," Porosh. Metallurgiya, No. 9-10, 46-51 (1994).
6. S. N. Lakiza, L. M. Lopato, L. V. Nazarenko, et al., "Liquidus surface for the $Al_2O_3-ZrO_2-Y_2O_3$ phase diagram," Ibid., No. 11-12, 39-43.
7. S. N. Lakiza, L. M. Lopato, and V. P. Smirnov, "Solidus surface and phase equilibria in crystallization of alloys in the $Al_2O_3-ZrO_2-Y_2O_3$ system," Ibid., No. 1-2, 71-76 (1995).
8. F. Schmid and D. Viechnicki, "Oriented eutectic microstructures in the system $Al_2O_3-ZrO_2$," J. Mater. Sci., **5**, No. 6, 470-473 (1970).
9. G. R. Fischer, L. J. Manfredo, R. N. McNally, et al., "The eutectic and liquidus in the $Al_2O_3-ZrO_2$ system," Ibid., **16**, No. 12, 3447-3451 (1981).
10. J. Echigoya, Y. Takabayashi, K. Sasaki, et al., "Solidification microstructure of Y_2O_3-added $Al_2O_3-ZrO_2$ eutectic," Trans. Jap. Inst. Metals, **27**, No. 2, 102-107 (1986).
11. A. V. Shevchenko, L. M. Lopatov, G. I. Gerasimyuk, et al., "The $HfO_2-ZrO_2-Al_2O_3$ system," Izv. AN SSSR, Neorgan. Mater., **26**, No. 4, 839-842 (1990).
12. V. S. Stubican, R. G. Hink, and S. P. Ray, "Phase equilibrium and ordering in the system $ZrO_2-Y_2O_3$," J. Amer. Ceram. Soc., **61**, No. 1-2, 17-21 (1978).
13. A. V. Shevchenko, V. D. Tkachenko, L. M. Lopato, et al., "A method of determining phase-transition temperatures by the use of solar heating," Porosh. Metallurgiya, No. 1, 91-95 (1986).
14. A. V. Shevchenko, L. M. Lopato, T. V. Obolonchik, et al., "The liquidus surface in the $HfO_2-ZrO_2-Y_2O_3$ system," Izv. AN SSSR, Neorgan. Mater., **23**, No. 3, 452-456 (1987).
15. N. A. Toropov, I. A. Bondar', F. Ya. Galakhov, et al., "Phase equilibria in the yttrium oxide-alumina system," Izv. AN SSSR, Ser. Khim., No. 7, 1158-1164 (1964).
16. D. Viechnicki and F. Schmid, "Investigation of the eutectic point in the system $Al_2O_3-Y_3Al_5O_{12}$," Mater. Res. Bull., 4, No. 2, 129-135 (1969).
17. J. L. Caslavski and D. J. Viechnicki, "Melting behavior and metastability of yttrium aluminium garnet (YAG) and $YAlO_3$ determined by optical differential thermal analysis," J. Mater. Sci., **15**, No. 7, 1709-1718 (1980).
18. I. A. Bondar', L. N. Koroleva, and E. T. Bezruk, "Physicochemical properties of yttrium aluminates and gallates," Izv. AN SSSR, Neorgan. Mater., **20**, No. 2, 257-261 (1984).
19. B. Cockayne, "The uses and enigmas of the $Al_2O_3-Y_2O_3$ phase system," J. Less-Common Met., **114**, No. 1, 199-206 (1985).
20. G. T. Adylov, G. V. Voronov, E. P. Mansurova, et al., "The $Y_2O_3-Al_2O_3$ system above 1473 K," Zh. Neorgan. Khimii, **33**, No. 7, 1867-1869 (1988).
21. Tail-Ih Mah and M. D. Petry, "Eutectic composition in the pseudobinary system of $Y_4Al_2O_9$ and Y_2O_3," J. Amer. Ceram. Soc., **75**, No. 7, 2006-2009 (1992).

THIS PAGE BLANK (U